PERGAMON

Vision Research 42 (2002) 2635–2644

Vision Research

www.elsevier.com/locate/visres

Fixation behavior while walking: persons with central visual field loss

Kathleen A. Turano *, Duane R. Geruschat, Frank H. Baker

The Johns Hopkins University School of Medicine, Wilmer Eye Institute, Baltimore, MD 21205, USA

Received 16 November 2001; received in revised form 6 June 2002

Abstract

The aim of this study was to determine the effect of central visual field loss (CFL) on fixation patterns of a person walking towards a target. Subjects were four visually normal persons and 10 persons with CFL. Eye position on scene was recorded and classified into 20 scene categories. The distributions of fixations among scene categories were compared across the two subject groups. For all but two CFL subjects, who fixated primarily at the floor, the distributions of fixations for the CFL subjects ranged from being moderately to strongly correlated with that of the visually normal mean. An analysis of the similarity in the sequence of fixations (or gaze pattern) of the CFL subjects to the visually normal subjects showed a range of 7–66%. Excluding the one CFL subject who had a functioning fovea, sequence similarity was strongly correlated with the logarithm of the minimum angle of resolution (log MAR). The better a person's log MAR, the more closely his or her gaze pattern matched that of the visually normal subjects. Finally, the CFL data were tested against two current models of oculomotor strategy, visual salience and guided search. Similar to what was found with visually normal subjects, CFL subjects appear to use the expected features and general location of the target to guide their fixations, the guided-search strategy.

Keywords: Mobility; Gaze; Vision impairment; Visual saliency; Guided search

1. Introduction

Until recently, technology limited the study of eye movements in mobile observers. As a consequence, little is known about the ways in which environmental information is explored while walking. A few studies have begun to address this issue with visually normal subjects (Hollands, Marple-Horvat, Henkes, & Rowan, 1995; Patla & Vickers, 1997; Turano & Geruschat, 2000, 2001; Turano, Geruschat, & Baker, submitted for publication). In a recent study, we showed that persons with normal vision walking to a predefined target directed their gaze primarily at objects in the environment that had features in common with the target. An oculomotor strategy that uses information about the expected features and general location of the target (guided-search model) [1] better matched subjects' gaze patterns (sequences of fixations) than a strategy in which gaze is directed at the most visually salient location in the retinal image (i.e., the visual salience model). For the visually normal person, saccadic eye movements direct the intended image to the fovea. Both visual acuity and contrast sensitivity decrease with increasing retinal eccentricity. For persons with long-standing central scotomas, preferred eccentric retinal loci are used for fixation, and non-foveating saccades direct the intended images to the eccentric retina (Cummings, Whittaker, Watson, & Budd, 1985; Timberlake et al., 1986; Whittaker, Budd, & Cummings, 1988, 1991). Non-foveating saccades have a longer latency and are less accurate than foveating saccades (Whittaker et al., 1991). Thus, eccentric retina is disadvantaged with respect to the fovea because of both poorer visual function and slower and inaccurate saccadic eye movements.

In this study we examined how central visual field loss (CFL) affects the ways in which information is explored as a person walks to a predefined target. One might predict that since persons with CFL have reduced visual acuity and contrast sensitivity, they would heavily depend on the most visually salient objects in the image to direct their gaze. Or it could be that since the cost of

* Corresponding author. Address: Lions Vision Center, 550 N. Broadway, 6th Floor, Baltimore, MD 21205, USA. Tel.: +1-410-502-6434; fax: +1-410-955-1829.

E-mail address: kathy@lions.med.jhu.edu (K.A. Turano).

[1] The guided-search strategy is based on the idea that information about the target differentially weights specific features that can bias the direction of gaze.

0042-6989/02/$ - see front matter
PII: S0042-6989(02)00299-7

redirecting gaze is high, in terms of time and accuracy, persons with CFL might try to maximize the efficiency of their search using top-down, cognitive cues about the target. Support for this hypothesis comes from a study conducted by Hayhoe and colleagues using visually normal subjects (Hayhoe, Ballard, & Whitehead, 1993). As the subjects performed a pattern-copying task, they repeatedly looked at the pattern while building the copy. However, when the pattern was placed farther away from the work area, making the gaze shift more expensive, they reduced their frequency of gaze shifts to the pattern, presumably relying more on memory. The study demonstrated that gaze strategy depends on the cost of redirecting gaze.

In our study, we recorded eye movements and calculated eye position relative to the scene. The percentage of fixations in various categories was computed, and the sequence of fixation categories (gaze patterns) was determined. Data from subjects with CFL were compared to the data obtained in a group of visually normal subjects. In addition, the gaze patterns of the CFL subjects were tested against the predictions of two current models of oculomotor strategy, visual salience and guided search.

2. Methods

2.1. Subjects

We tested 10 subjects with diagnosed CFL: five with age-related macular degeneration (AMD) and five with Stargardt's or juvenile macular degeneration. Their data were compared to that of four visually normal subjects (uncorrected or corrected binocular visual acuity better than 20/25 and binocular log peak contrast sensitivity better than 1.65). Any subject with self-reported physical limitations (e.g., orthopedic), cognitive limitations (e.g., Alzheimer's disease), or health limitations (e.g., heart condition), was excluded from participation. All subjects walked without assistance and without any mobility aid or device. Informed consent was obtained from each subject after the nature and possible consequences of the study were described. The research was approved by the Johns Hopkins Medical Institution committee on human experimentation. Table 1 lists the ages, visual function measures, and travel times of the subjects.

2.2. Mobility task

The mobility route consisted of the corridors of a floor in an office building that had never been seen by any of the subjects. An experimenter followed the subject throughout the route and recited standardized directions at specified points along the way. Each subject was told to walk safely, at his or her normal pace, following the instructions given. The instructions for the section of the route analyzed for this study were "As you walk down this hall, find the fifth door on the left and turn to go through". The distance for this section of the route was 24.8 m.

2.3. Visual function measures

Visual acuity was measured binocularly in all subjects using a Lighthouse ETDRS acuity chart (Ferris, Kass-

Table 1
Subject characteristics

Subject	Age (years)	Diagnosis	Log MAR	Log CS	Size of scotoma (deg)	SD of central gaze[a] (deg, H)	SD of central gaze (deg, V)	r^b	Similarity score (%)	Travel time (s)
NPD	49.4	Normal vision	−0.16	1.7	–	0.34	0.27	–	–	21.3
NJF	57.8	Normal vision	−0.06	1.9	–	0.36	0.14	–	–	27.2
NEL	66.2	Normal vision	0.04	1.7	–	0.29	0.26	–	–	23.8
NLT	36.2	Normal vision	−0.12	1.9	–	0.28	0.24	–	–	19.3
AFW	84.3	AMD	1.06	1.05	19 × 15	1.10	1.27	0.1	24	32.3
AGJ	77.0	AMD	0.56	1.1	9 × 13	0.71	0.33	0.89	66	25.6
AHF	70.5	AMD	0.80	0.7	17 × 12	0.21	0.60	0.77	64	23.4
ARB	71.0	AMD	0.74	1.3	5 × 3	0.45	0.85	0.53	41	22.7
ASK	78.5	AMD	0.60	1.6	8 × 3	0.12	0.16	0.93	63	22.0
SAM	17.2	Stargardts	0.90	1.6	3 × 3	0.29	0.39	0.54	31	31.9
SMA	45.5	Stargardts	0.18	1.4	8 × 8[c]	0.20	0.33	−0.02	7	25.6
SMS	19.8	Stargardts	0.94	1.1	7 × 5	0.34	0.45	0.45	38	22.0
SMZ	25.1	Stargardts	0.20	1.65	2 × 2	0.30	0.19	0.88	59	22.2
SRS	27.8	Stargardts	1.30	1.5	13 × 13	0.34	0.83	0.47	24	22.4

[a] Gaze stability estimated as SD of gaze when looking at central fixation point in calibration.
[b] Correlation coefficient of CFL subject's fixation distribution and the distribution of the visually normal mean.
[c] Central sparing of 3° × 3°.

off, Bresnick, & Bailey, 1982) transilluminated at 95 cd/m^2. Visual acuity was scored as the number of letters correctly read, and was converted to log MAR (the logarithm of the minimum angle of resolution) in the manner specified by Bailey, Bullimore, Raasch, and Taylor (1991). Peak contrast sensitivity was measured binocularly in all subjects using the Pelli-Robson chart (Pelli, Robson, & Wilkens, 1988) with overhead illumination (approximately 85 cd/m^2) at a viewing distance of 1 m. Log peak CS is the logarithm of the reciprocal of the contrast threshold value. Scotoma size and retinal fixation location was measured monocularly in each eye of the subjects with CFL by static perimetry using the confocal scanning laser ophthalmoscope (SLO) equipped with graphics capabilities (Webb, Hughes, & Delori, 1987). This system obtains retinal images continuously with an infrared laser. At the same time, graphics are scanned onto the retina with a modulated visible laser and viewed by the subject. We used the landmark-driven fundus perimetry technique developed by Sunness et al. (1995) that compensates for eye movements. Each eye was tested with a 10 minarc square of retinal illuminance 7×10^4 Trolands (the laboratory's standard SLO perimetric probe to test for dense scotomas). We calculated the size and position of binocular scotomas by assuming the subjects used the monocular retinal location in each eye when fixating binocularly. A binocular scotoma was defined as the scotomatous area common to both eyes, determined by overlaying the monocular retinal images with the retinal fixation locations anchored. The estimated size of each CFL subject's binocular scotoma is listed in Table 1. As shown the sizes of the binocular scotomas ranged from $2° \times 2°$ to $19° \times 15°$. Schematics of three subjects' left retinas superimposed with their estimated binocular scotomas (black rectangles) and preferred retinal location for fixation (marked by X's) are shown in the left column of Fig. 1.

2.4. Eye-on-scene recording

We used the ISCAN (ETL-410), a headband-mounted eye tracking system, to obtain images of the eye and scene. Our system was modified to be battery operated and had a wide-lens scene camera to provide an

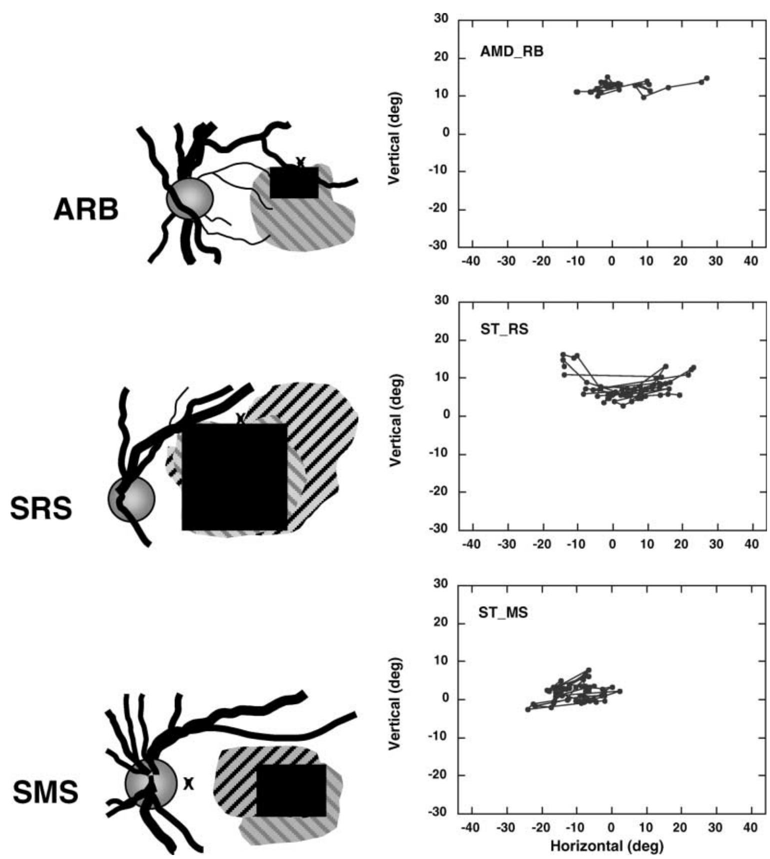

Fig. 1. Schematic of three subjects' left retinas (left column) adapted from SLO measurements. Superimposed on each retina is the left eye scotoma (left hatched area), right eye scotoma (right hatched area), estimated binocular scotoma (black rectangles) and preferred retinal locus (indicated by an X). Estimates are from SLO perimetry. Circuitous lines illustrate part of the retinal vasculature, and the optic disk of the left eye is shown as a solid circle. (To approximate the scale, an optic disk diameter is roughly 5°.) The right column shows the fixation locations (eye relative to the scene camera) for the same three subjects. The center coodinates (0° H, 0° V) represent fixation straight ahead. Negative x-axis values indicate positions left of straight ahead, and negative y-axis values refer to positions below straight ahead.

$88^\circ \times 60^\circ$ field of view. The cameras' outputs were recorded on digital video camcorders (Canon ZR10) carried in a backpack and analyzed offline. The camcorders were synchronized by simultaneously recording a tone on the audio channels of the two camcorders. The eye and scene images were recorded at 30 frames/s. At the beginning of the experiment the subject donned a silicon swim cap to ensure positional stability of the eye-tracker and then the eye-tracker headband was fitted on the subject's head. Next the eye-tracker was calibrated by having the seated subject sequentially fixate each of five points of a calibration pattern, while on a bitebar. (Calibration accuracy for each subject is estimated from the SD of gaze position obtained during 5 s of looking at the central fixation point and is listed in Table 1.) The recorded eye images were used in offline analysis to relocate ISCAN eye-position values to direction of gaze. Upon completion of the mobility data collection, the eye recording was fed into the ISCAN processing board that was externally triggered by the synchronizing tone. The ISCAN software uses the pupil and corneal reflection to identify the angular position of the eye. The scene recording used a video capture board (Broadway by Data Translation) whose software was modified to trigger on the synchronization tone on the videotape. In-house software was developed to transform the eye position data in ISCAN units to screen coordinates and to adjust eye position in accordance with the barrel distortion of the image introduced by the scene camera of the ISCAN system. To compensate for the barrel distortion, we used a lookup table based on the actual measured degree of distortion across the image. Movies of the eye-on-scene were made for each subject, and a graphic character was superimposed on each frame of the movie at the calculated eye position. The spatial resolution of the images was 0.25° per pixel.

Fixations were identified using a velocity threshold of eye position relative to a scene landmark. To do this, for each frame of the scene movie, the coordinates of a distant stationary landmark were digitized and stored. The change in the distance between the eye and the landmark was computed across consecutive frames. A fixation was defined as a change less than 1.6°, which is equivalent to the eye-on-scene remaining within 1.6° for two frames (i.e., 67 ms), or a velocity slower than 25°/s.

The right column of Fig. 1 shows the fixations of three subjects while walking the first half of the mobility route. The fixations are depicted in terms of horizontal and vertical positions relative to the scene camera (which was attached to the subject's head). The coordinates 0° H and 0° V indicate fixation straight ahead. The negative values on the x-axis refer to left of straight ahead and the positive values, right. The negative values on the y-axis refer to below straight ahead and positive, above. A comparison across the three graphs shows the difference in fixation locations of the three subjects. Subject ARB maintained a fairly constant vertical level with his eyes whereas subject SMS showed more variation vertically and less horizontally. The left side of Fig. 1 shows schematics of the left retinas of the three subjects. Superimposed on the schematics are the estimated binocular scotomas (black rectangles) and preferred retinal locations (X's). The preferred retinal location of subject ARB is just above the scotoma (which corresponds to fixating just *below* the scotoma in the visual field). The same is true for subject SRS. Whereas, the preferred retinal location of subject SMS is a retinal location more than 5° to the left of the binocular scotoma. A visual inspection of the fixations of all the CFL subjects showed no apparent association with scotoma size or location.

2.5. Analysis

We used a categorical analysis to analyze the data (Choi, Mosley, & Stark, 1995; Stark & Choi, 1996). Twenty categories were defined according to meaningful partitions (e.g., floor, ceiling, target) and each assigned a letter. The position of eye-on-scene at each fixation (identified using a velocity threshold of 25°/s) was classified into one of the 20 categories, producing a sequence of letters that indicated the fixation positions.

A sequence alignment analysis (CLUSTALW from the MacVector software by Oxford Scientific) was used to quantify the similarity between gaze patterns. The analysis determined the optimal alignment between datasets being compared, maintaining the order of categories within the sequences. The program can shift sequences with respect to one another and/or add blanks to obtain the optimal alignment. We computed the optimal alignment for the data of each CFL subject to the data of all four visually normal subjects. The percentage of matched categories (similarity score) between the datasets of each CFL subject and the visually normal subjects was calculated. (A match was counted when the same category occurred in the sequences of the CFL subject and at least two visually normal subjects.) Fig. 2 provides an illustration of a sample sequence alignment output. Gray boxes indicate matched pairs. The data are of subject AGJ and the visually normal subjects. The similarity score for AGJ was 66% (76 matches/116 fixations), indicating that two-thirds of his sequence (gaze pattern) matched the sequences of the visually normal subjects.

2.6. Models

For the visual salience model, we used a computer implementation of a model developed by Itti, Koch, and Niebur (1998). With this model, feature maps (intensity, color, and orientation) are computed by a set of center-surround operations performed across spatial scales. The three resulting maps are summed to create a single

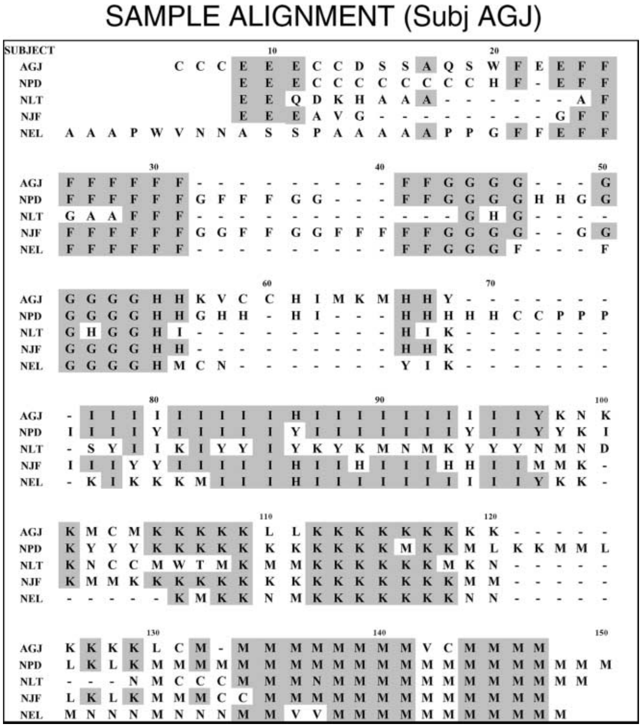

Fig. 2. Sample of sequence alignment output. Gray boxes indicate matched pairs. (A match was counted when the same category occurred in the sequences of the CFL subject and at least two visually normal subjects.) Data are of subject AGJ and the visually normal subjects. Similarity score for AGJ was 66% (76 matches/116 fixations), indicating that two-thirds of his sequence (gaze pattern) matched the sequences of the visually normal subjects. Key for the category codes is found on the horizontal axis in Fig. 4.

saliency map. The most salient location determines the location of the next fixation. For the guided-search model, the visual salience model was modified such that the parameters that weight the target features were increased to bias the features common to the target. In the present study the weights of the features, "vertical" and "large", were increased and spatial location was restricted to the left side of the image. Model predictions of fixation location were computed from the video frames of each subject's fixations and categorized in the manner described above for the eye data.

3. Results

Fig. 3 shows pictures of the scene with superimposed alphanumeric characters to indicate the fixation locations of the CFL subjects (AMD subjects, left panel; Stargardt's subjects, right panel). The data were collected in the first 7.5 s. Data collected beyond 7.5 s are counted in the analysis but not displayed here. The complete eye-on-scene recordings of the CFL and visually normal subjects can be seen by viewing the movies at http://162.129.125.249/gaze.html. In the movies, a red cross superimposed on the scene indicates the eye position, and a blue cross indicates a blink. For the CFL subjects, a rectangle of the approximate size of the binocular scotoma is positioned relative to fixation as determined by the SLO.

A comparison across subjects illustrates the degree of variability in the data of the CFL group. To illustrate, subjects AGJ and SRS fixate on both the left and right sides of the scene, whereas, subject SMS fixates exclusively on the left side. These data contrast with those of subjects AFW and SMA where the majority of the fixations are directed at the floor.

Fig. 4 shows the distribution of fixations across the scene categories for the group of CFL subjects. The bars indicate the mean, and the error bars represent 1 standard deviation. The labels on the horizontal axis are the scene categories with the lower axis showing abbreviated category names and the upper axis showing category codes that serve as keys for the labels in Figs. 2 and 5. Multiple occurrences of a category are coded by an "L" or "R" suffix, to indicate side of scene, followed by a number to indicate order of occurrence relative to the beginning of the route. For example, "doorL1" indicates the first left-side door and "wallL23" indicates the wall on the left side between the second and third doors. (The wall categories include any existing posters on the walls.) The results showed that the category "floor" had the most fixations; the mean percentage for the CFL group was 21%. The large variability in this category, shown by a standard deviation of 24.2%, indicates that not all CFL subjects had a high percentage of fixations in the category "floor". This can be observed in the individual representations of fixation locations (shown in Fig. 3). The scene category "target" had the second most fixations, with a mean percentage of 15.8% (SD = 10.6%). Other popular categories were the left-side doors, posters and walls.

Pearson product correlation analyses were performed on each CFL subject's percentage of fixations per category and the percentage of fixations of the visually normal mean. All correlations were significant except for the data of subjects AFW and SMA. Of those that were significant, the correlation coefficients ranged from 0.45 to 0.93 (correlation coefficients are listed in Table 1). These values indicate a moderate-to-high degree of association between the distributions of the CFL subjects and the visually normal mean. For the most part, the CFL subjects had a lower percentage of fixations in the "left door" categories compared to the visually normal subjects. A few CFL subjects (AFW, SAM, and SMA) had a significantly higher percentage of fixations in the "floor" category.

A hierarchical clustering analysis was performed on the CFL subjects' data to determine whether there was an obvious pattern in fixation frequency for the various categories. Hierarchical clustering is a multivariate

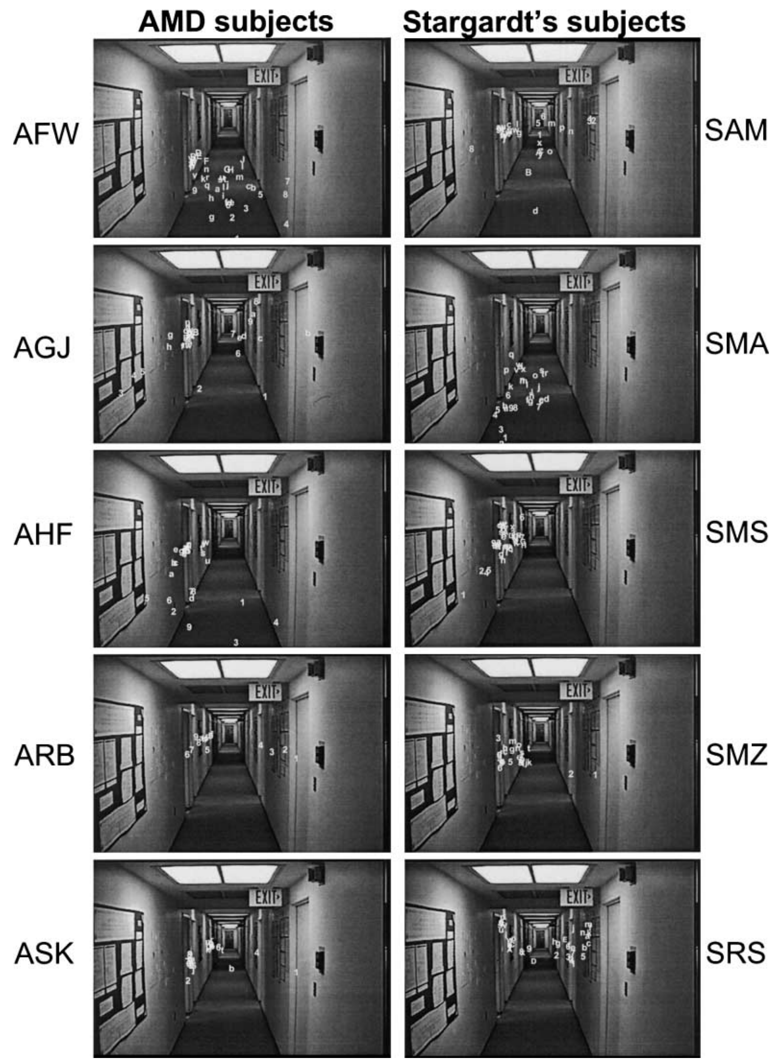

Fig. 3. Pictures of the scene with superimposed alphanumeric characters illustrating the eye-on-scene locations for the fixations of the CFL subjects. Left panel shows data of the AMD subjects and the right panel, data of the Stargardt's subjects. Fixation order is coded by the sequence: 1–9, a–z, A–Z.

technique that groups together elements that have similar values. In our case the categories with similar fixation percentages were grouped together. The process starts with each element as its own cluster and the distance between each cluster is calculated. The two clusters that are closest together are combined and the process reiterates until all points are in a final cluster. The clustering tree can be cut at various points. A cut at four in the CFL subjects' data produces the following pattern. The floor and the target each formed their own cluster. Another cluster consisted of the first four left-side doors and left-side posters/walls (wallL23, wallL34). The last cluster consisted of all other categories.

The grouping pattern of fixation percentages is easily identifiable in the graphs of Fig. 5. The symbols represent the clusters that were identified in the hierarchical clustering analysis. The spread of points along the horizontal axis shows the fixation percentages of the CFL subjects. The categories "floor" (indicated by "C") and "target" (indicated by "M") have the most fixations and are clearly isolated from the rest. The next most fixated categories, left-side doors, posters, and walls are clustered between 5% and 10%. The remaining categories cluster together on the left side of the graph, the side of the lowest percentages.

In Fig. 5a, the predicted fixation percentages of the visual salience model are plotted against the actual fixation percentages. The correlation coefficient for the two distributions was 0.28, ns, indicating no significant linear relationship between the predictions of the visual salience model and where the CFL subjects looked while walking. In Fig. 5b, the predicted fixation percentages of the guided-search model are plotted against the actual fixation frequencies. The correlation coefficient for the two distributions was 0.80, $p < 0.01$. A fairly strong linear relationship exists between the predicted fixation locations of the guided-search model and where the subjects looked while walking.

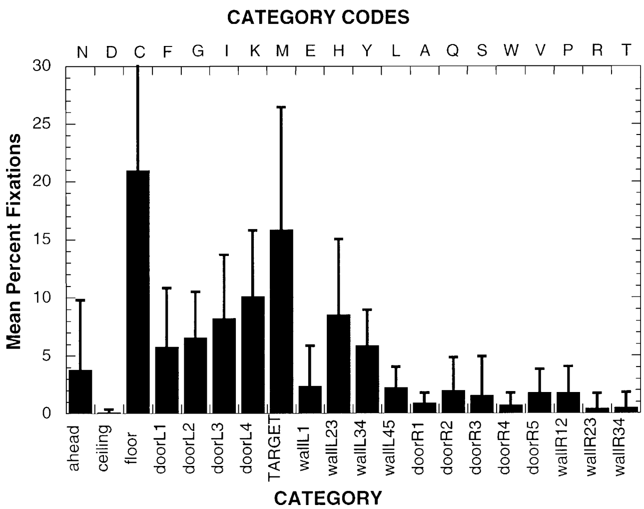

Fig. 4. Distribution of fixations among scene category for the group of CFL subjects. The bars indicate the mean, and error bars represent 1 standard deviation. The labels on the horizontal axis are the scene categories, with labels on the lower axis showing abbreviated category names and labels on the upper axis showing category codes to serve as keys for labels in Figs. 2 and 5. Multiple occurrences of a category are coded by an "L" or "R" suffix, to indicate side of scene, followed by a number to indicate order of occurrence relative to the beginning of the route. For example, "doorL1" indicates the first left-side door and "wallL23" indicates the wall on the left side between the second and third doors. (The wall categories include any existing posters on the walls.)

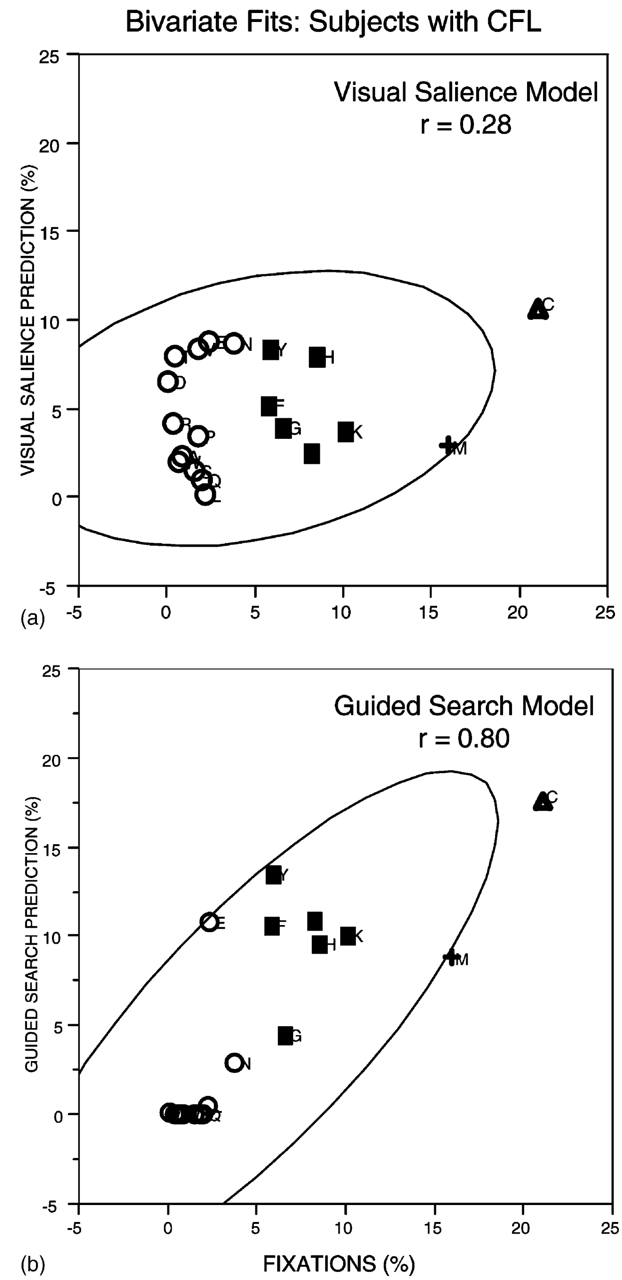

Fig. 5. (a) Predicted fixation percentages from the visual salience model and the (b) guided-search model plotted against the actual fixation frequencies. The symbols represent the clusters that were identified in the hierarchical clustering analysis. Bivariate normal density ellipses show where 95% of the data are expected to lie. The correlations between the predicted frequency of fixations of the models and the actual frequencies are shown in the upper right corners.

The bivariate fits of the models' predictions to the data are shown as normal density ellipses (95% confidence interval) on the graphs. The "floor" is the only category that falls outside the ellipse in both models.

In the previous section, we showed comparisons of fixation percentages per scene category between the CFL and visually normal subjects as well as between each CFL subject and the models' predictions. In those analyses the percentage of fixations in each category (e.g., floor) did not rely on the order in which the fixations were executed (e.g., first "doorL1", second "doorL2", third "doorL1"...). In the next section, we report the results of an analysis in which the order of fixations mattered. We determined the similarity in gaze patterns between each CFL subject and the visually normal subjects. The similarity scores were derived in the manner described in Section 2.5 and are listed in Table 1. The similarity scores ranged from 7% to 66%.

Somewhat surprising was the finding that the lowest score was from the one CFL subject who had a functioning fovea. Subject SMA has a bulls-eye scotoma: an $8° \times 8°$ central scotoma with a spared central $3° \times 3°$ region. To determine whether the large amount of variability in the similarity scores of the CFL subjects is a reflection of the variation in visual function or age within the group, we computed the correlations between subject characteristics and similarity scores. (Subject SMA was excluded in the analysis because of her idiosyncratic foveal sparing.) From a power analysis we determined that with our sample size of 9 we are able to detect, at a 0.05 significance level, a correlation of 0.7 or higher, with a power of 0.75 (Cohen, 1988). We analyzed the subject characteristics age, log MAR, log CS, scotoma diameter, and travel time and found a significant correlation between log MAR and the similarity score ($r = -0.79$). No other subject characteristic was

Table 2
Correlation coefficients of CFL subject characteristics and percentage gaze pattern similar to normals

Subject characteristic	r
Age	0.36
Log MAR	−0.79*
Log CS	−0.153
Scotoma diameter (H)	−0.175
Scotoma diameter (V)	−0.177
Travel time	−0.46

*$p < 0.01$.

significantly correlated with the similarity score (Table 2). Fig. 6 shows the relationship between the similarity scores and log MAR. As log MAR increases (or visual acuity decreases) the less similar the CFL subjects' gaze patterns are to those of the visually normal subjects.

In the sections above, we reported the estimates of similarity in fixation behavior between the CFL subjects and the visually normal subjects using two measures. The first measure was the correlation coefficient, r, for the distributions of fixation percentages, and the second measure was the similarity scores for the gaze patterns. To determine whether one measure predicts the other, we regressed similarity score on r. The results showed that r could explain 88% of the similarity score variance, $R^2 = 0.88$, $p < 0.01$. Similarity score $= 0.09 + 0.58r$. In other words, the estimate of similarity with the visually normal subjects with respect to the *sequence* of fixations can be calculated from the degree of association in a person's fixation distribution.

4. Discussion

The goal of this study was to determine how CFL affects visual exploratory behavior while walking toward a target. People with CFL often fixate with eccentric retina, which has decreased visual function and compromised saccadic control, suggesting that exploratory behavior may be affected. We recorded eye movements and calculated eye position relative to the scene in persons with CFL and in visually normal persons. Eye position on scene was then classified into one of 20 categories. Visual exploratory behavior was assessed in two ways. One, the distribution of fixations per category was calculated to indicate where in the scene a subject fixated, and two, the order in which a subject executed those fixations (gaze pattern) was determined.

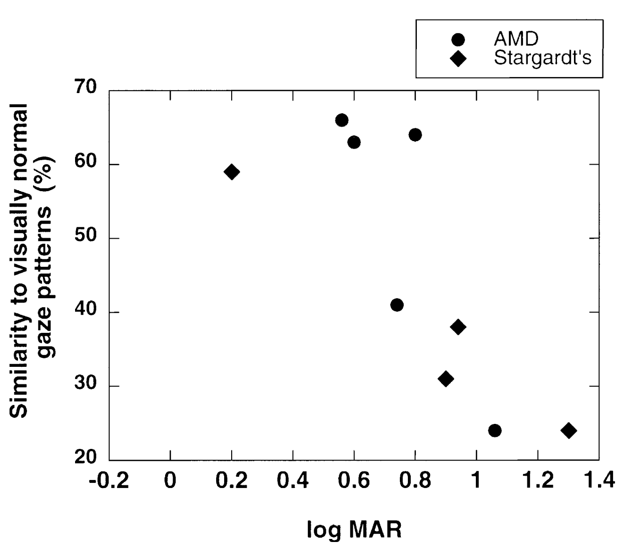

Fig. 6. Similarity scores of the CFL subjects' gaze patterns plotted against log MAR.

4.1. Where in the scene do CFL subjects look while walking?

The distribution of fixations per scene category was calculated for the CFL group and is shown in Fig. 4. From this graph one might think that the CFL subjects fixated primarily on the floor, a view in concordance with clinical impression. However, this is true for only a few CFL subjects. The individual distributions show that only subjects, AFW, SAM, and SMA, fixated predominately on the floor. Three other subjects fixated predominately on the target and two others, on the fourth left door. The results from a hierarchical clustering analysis indicated that, apart from the floor and target, the CFL group fixated mostly on left-side posters and walls. As a whole, the CFL group made few fixations to the ceiling, ahead, and right-side doors, posters and walls. However, as shown in the illustrations in Fig. 3, two subjects (AGJ, SRS) did fixate on the right side.

One reason that subjects might direct their fixation at the floor is that they are afraid of falling and therefore attempt to maximize their detection of drop-offs. Previous to the mobility task, the subjects had been administered a questionnaire that included mobility-related questions. One question was "Have you had a fear of falling in the last year?" To test the hypothesis that those who have a fear of falling fixate the floor to a greater extent than those who do not, a t-test was performed on the percentage of floor-directed fixations. The results showed that those who reported a fear of falling had a significantly higher percentage of floor-directed fixations (mean = 47.3%) than those who did not (mean = 9.7%, $t(8) = -3.20$, $p = 0.01$), suggesting that the psychological factor, fear of falling, is related to visual exploratory behavior.

4.2. Fixation behavior of the CFL subjects compared to that of the visually normal subjects

The visually normal subjects fixated primarily on the target, followed by the left-side doors "K", "I", and "F". In our study, subjects were given instructions to walk to a specific target—the fifth door on the left. The visually normal subjects directed the majority of their fixations on the side of the scene of the target and more specifically at the left-side doors that were candidate targets. The distribution of the visually normal mean was compared with the distributions for each of the CFL subjects. The distributions of two CFL subjects, AFW and SMA, showed no association with the visually normal distribution (see the ninth column of Table 1). The degree of association for the distributions of the remaining CFL subjects ranged from moderate ($r = 0.45$) to high ($r = 0.93$).

The variation in degree of association between the fixation distributions of the CFL subjects and the visually normal mean was mirrored in the variation of similarity scores in the gaze patterns (where the *sequence* of fixations matters). The CFL similarity scores ranged from 7% to 66%. Those who fixated on the same categories as the visually normal subjects tended to have the same sequence of fixations as they did.

4.3. Similarity in gaze patterns of the CFL subjects to the visually normal relates to logMAR

The similarity scores for the gaze patterns of the CFL subjects, excluding the one CFL subject who had a functioning fovea, were correlated with log MAR ($r = -0.79$). (The correlation coefficients of the fixation distributions were also correlated with log MAR, $r = -0.75$.) The lower a CFL subject's visual resolution the greater the deviation in fixation behavior from that of the visually normal subjects. Log MAR is an estimate of the resolving power of the visual system, but it also depends on the distance between the region of fixation and the fovea. It is possible that this latter factor may actually be more responsible for the deviation in visual exploratory behavior than the drop in visual resolution per se.

The correlation between scotoma size and similarity score ($r = -0.18$) was not as high as its correlation with log MAR ($r = -0.79$). In our study the size of scotoma was only moderately correlated with log MAR (0.50). For some subjects the scotoma was not centered on the fovea, and, for other subjects, fixation was not juxtaposed to the scotoma (e.g., subject SMS, shown in Fig. 1).

4.4. Guided-search model better predicts the gaze strategy of the CFL subjects

In the introduction we posited hypotheses regarding the oculomotor strategy that would better predict the fixation behavior of the CFL subjects. One argument stated that persons with CFL might rely heavily on the visual salience of the scene to guide fixations because their visual function (e.g., visual acuity and contrast sensitivity) is compromised. Therefore the visual salience strategy would better predict the CFL subjects' fixations. The other argument stated that persons with CFL might rely heavily on cognitive or top-down information to direct their gaze because visual information, overall, is compromised. According to this view, the guided-search strategy would better predict behavior. The results showed the latter alternative to be true; the guided-search model was a better predictor of the gaze patterns. The predicted fixation percentages per category were highly correlated with the fixation percentages of the CFL group. The strength of the linear relationship between the two factors was 0.8.

The predictive power of the guided-search strategy could be further improved by including a component that was dependent on psychological factors. In this particular study, biasing the direction of gaze downward if the person had a reported fear of falling would have increased the percent similarity between model and data. As the database of gaze patterns grows, hopefully the knowledge of the relationship between gaze behavior and psychological factors will increase. These can then be incorporated into oculomotor strategy models.

In summary, we explored the fixation behavior of subjects with CFL and compared it to the fixation behavior of visually normal subjects. We looked at where in the scene subjects fixated (fixation distributions) as well as the order in which objects were fixated (gaze patterns). The CFL subjects showed a wide range in the degree of similarity in fixation behavior to the visually normal subjects. A visual measure that was strongly correlated to the degree of similarity was log MAR. The better a person's log MAR, the more closely their gaze pattern matched that of the visually normal subjects. Finally, we compared the predictions of two oculomotor strategies (visual salience and guided search) against the fixation data of the CFL subjects and found the guided-search model to be a better predictor of CFL performance.

Acknowledgements

This research was supported by the National Institutes of Health, National Eye Institute, under grant EY07839 to KAT. The authors thank Julie Stahl for her role in data collection and analysis, Marc Shapiro and Claudius Li for software development, and Frank Turano for the sequence analyses.

References

Bailey, I. L., Bullimore, M. A., Raasch, T. W., & Taylor, H. R. (1991). Clinical grading and the effects of scaling. *Investigative Ophthalmology and Visual Science, 32*, 422–432.

Choi, Y. S., Mosley, A. D., & Stark, L. W. (1995). String editing analysis of human visual search. *Optometry and Vision Science, 72*, 439–451.

Cohen, J. (1988). *Statistical power analysis for the behavioral sciences* (2nd ed.). Hillsdale, NJ: Lawrence Erlbaum Associates, Publishers.

Cummings, R. W., Whittaker, S. G., Watson, G. R., & Budd, J. M. (1985). Scanning characters and reading with a central scotoma. *American Journal of Optometry and Physiological Optics, 62*, 833–843.

Ferris, F. L., Kassoff, A., Bresnick, G., & Bailey, I. (1982). New visual acuity charts for clinical research. *American Journal of Ophthalmology, 94*, 91–96.

Hayhoe, M. M., Ballard, D. H., & Whitehead, S. D. (1993). Memory use during hand-eye coordination. *Proceedings of the Cognitive Science Society, 15*.

Hollands, M. A., Marple-Horvat, D. E., Henkes, S., & Rowan, A. K. (1995). Human eye movements during visually guided stepping. *Journal of Motor Behaviour, 27*, 155–163.

Itti, L., Koch, C., & Niebur, E. (1998). A model of saliency-based visual attention for rapid scene analysis. *IEEE Transactions on Pattern Analysis and Machine Intelligence (PAMI), 20*, 1254–1259.

Patla, A. E., & Vickers, J. N. (1997). Where and when do we look as we approach and step over an obstacle in the travel path? *Neurophysiology, 8*, 3661–3665.

Pelli, D. G., Robson, J. G., & Wilkens, A. J. (1988). The design of a new letter chart for measuring contrast sensitivity. *Clinical Vision Sciences, 2*, 187–199.

Stark, L., & Choi, Y. S. (1996). Experimental metaphysics: The scanpath as an epistemological mechanism. *Visual Attention and Cognition*.

Sunness, J. S., Schuchard, R. A., Shen, N., Rubin, G. S., Dagnelie, G., & Haselwood, D. M. (1995). Landmark-driven fundus perimetry using the scanning laser ophthalmoscope. *Investigative Ophthalmology and Visual Science, 36*, 1863–1874.

Timberlake, G. T., Mainster, M. A., Peli, E., Augliere, R. A., Essock, E. A., & Arend, L. E. (1986). Reading with a macular scotoma. I. Retinal location of scotoma and fixation area. *Investigative Ophthalmology and Visual Science, 27*, 1137–1147.

Turano, K. A., & Geruschat, D. R. (2000). Gaze patterns during mobility are repetitive and idiosyncratic in both normal and vision-impaired persons. *Investigative Ophthalmology and Visual Science, 41*(Suppl.), S814.

Turano, K. A., & Geruschat, D. R. (2001). Visual scan patterns while walking challenge the random-walk and visual-salience oculomotor scanning strategies for persons with and without a fovea. *Investigative Ophthalmology and Visual Science, 42*(Suppl.), S927.

Turano, K. A., Geruschat, D. R., & Baker, F.R. (submitted for publication). Oculomotor strategies for the direction of gaze tested with a real-world activity.

Webb, R. H., Hughes, G. W., & Delori, F. C. (1987). Confocal scanning laser ophthalmoscope. *Applied Optics, 26*, 1492–1499.

Whittaker, S. G., Budd, J. M., & Cummings, R. W. (1988). Eccentric fixation with macular scotoma. *Investigative Ophthalmology and Visual Science, 29*, 268–278.

Whittaker, S. G., Cummings, R. W., & Swieson, L. R. (1991). Saccade control without a fovea. *Vision Research, 31*, 2209–2218.